

Compatibility of the Updated $(g - 2)_\mu$, $(g - 2)_e$ and PADME-Favored Couplings with the Preferred Region of ATOMKI X17

Emrys Peets^{*1,2}

¹Department of Physics, Stanford University, Stanford, CA 94305, USA

²Fundamental Physics Directorate, SLAC National Accelerator Laboratory, Menlo Park, CA 94025, USA

February 3, 2026

Abstract

We re-evaluate the viability of a kinetically mixed dark photon (A') as a solution to the muon anomalous magnetic moment $(g - 2)_\mu$ discrepancy and the ATOMKI nuclear anomalies near 17 MeV, using the final FNAL measurement and the latest theory predictions (BMW21, WP25). For $m_{A'} = 17$ MeV, the allowed kinetic mixing parameter narrows to $\varepsilon_\mu = 7.03(58) \times 10^{-4}$ (WP25). We then directly compare the allowed region for the muon and X17 bands to those preferred by the electron magnetic moment measurements. For the electron, we obtain $\varepsilon_e = 1.19(15) \times 10^{-3}$ (Cs, 2018) and $\varepsilon_e = 0.69(15) \times 10^{-3}$ (Rb, 2020), based on two recent measurements of the fine structure constant compared to the most recent experimental value determined using a one-electron quantum cyclotron. This study focuses on the protophobic vector interpretation of X17 and assumes $\varepsilon_\nu \ll \varepsilon_l$. While a mild tension persists, we identify a narrow overlapping region, $6.8 \times 10^{-4} \lesssim \varepsilon \lesssim 9.6 \times 10^{-4}$, between recent PADME results, the NA64 exclusion, and within the 2σ preferred coupling region given by the Rb 2020 determination of α_e . These results provide well-defined targets for future experimental searches and motivate further theoretical refinements, both of which will play a decisive role in assessing the validity of the ATOMKI anomaly claims. Of particular note is the fixed target X17 experiment to be conducted in Hall-B of Thomas Jefferson National Accelerator Facility in Summer of 2026.

1 Introduction

Light, weakly-coupled spin-1 mediators arise naturally in extensions of the Standard Model by an additional $U(1)$ gauge factor, where the associated gauge boson X_μ can interpolate between a dark-photon-like state (coupled dominantly to Q via kinetic mixing), a dark- Z -like state (via Z - X mixing), and more general forces coupled to linear combinations of Q , B , and L (or B - L). In a generic low-energy effective description one may write

$$\mathcal{L} \supset -\frac{1}{4}X_{\mu\nu}X^{\mu\nu} + \frac{1}{2}m_X^2X_\mu X^\mu + X_\mu \sum_f \bar{f}\gamma^\mu \left(g_V^f + g_A^f \gamma^5 \right) f, \quad (1)$$

where g_V^f and g_A^f are the vector and axial couplings to SM fermions. In ultraviolet completions with extra Higgs structure (e.g. multiple doublets plus singlets), the effective $U(1)$ current can contain both vector and axial pieces, and the vector part may be arranged to be approximately “protophobic”—i.e. the effective proton coupling is suppressed compared to the neutron coupling [1, 2, 3, 4]. At the quark level this is expressed as

$$g_V^p \equiv 2g_V^u + g_V^d, \quad g_V^n \equiv g_V^u + 2g_V^d, \quad |g_V^p| \ll |g_V^n|, \quad (2)$$

*Corresponding author: epheets@stanford.edu

with a particularly natural realization from Z - X mixing yielding a small ratio g_V^p/g_V^n (set by electroweak charges) [1]. Such a protophobic, MeV-scale vector has been widely discussed in connection with the ATOMKI e^+e^- angular-correlation anomalies [5, 6]. In this work we focus on the protophobic-vector interpretation and adopt the neutrino-suppressed benchmark $|g_\nu| \ll |g_e|$ (equivalently $|\epsilon_\nu| \ll |\epsilon_e|$ in mixing language), as motivated by neutrino-scattering constraints [7].

A central phenomenological handle on such light vectors is the one-loop contribution to lepton magnetic moments, which cleanly separates vector and axial pieces and highlights why axial couplings are typically much more tightly constrained at low mediator mass [8]. Writing the charged-lepton couplings as $f_{\ell V} \equiv g_V^\ell$ and $f_{\ell A} \equiv g_A^\ell$, one finds model contributions to a_ℓ of

$$\delta a_\ell \simeq \frac{f_{\ell V}^2}{8\pi^2} G\left(\frac{m_X}{m_\ell}\right) - \frac{f_{\ell A}^2}{4\pi^2} \frac{m_\ell^2}{m_X^2} H\left(\frac{m_X}{m_\ell}\right), \quad (3)$$

with loop functions that may be written as the Feynman-parameter integrals

$$G(r) = 2 \int_0^1 dx \frac{x^2(1-x)}{x^2 + r^2(1-x)}, \quad (4)$$

$$H(r) = \int_0^1 dx \frac{2x^3 + (x-x^2)(4-x)r^2}{x^2 + (1-x)r^2}, \quad (5)$$

so that for $r \ll 1$ one has $G(r) \rightarrow 1$ and $H(r) \rightarrow 1$ while the axial term is enhanced by the explicit factor m_ℓ^2/m_X^2 [8]. In the dark-photon limit (purely vector, flavor-universal coupling) one may identify $f_{\ell V} = e\epsilon$ and $f_{\ell A} = 0$, recovering the familiar $\delta a_\ell \propto \alpha\epsilon^2$ scaling used throughout dark-sector phenomenology [9, 4]. This tight interplay between $(g-2)_\ell$, nuclear-transition kinematics, and protophobic charge assignments motivates targeted tests of the remaining MeV-scale parameter space.

This Study

Using the latest results from the (g-2) experiment [10], and considering BMW lattice QCD corrections to the gyromagnetic ratio to the muon [11], we report updated allowed parameter space for dark sector heavy photons between masses of 5 and 500 MeV that could couple to muons. We include the first comparison of the $(g-2)_\mu$ allowed ϵ and the preferred coupling given the ATOMKI measurements [12, 13, 14]. We illustrate how the theoretical prediction of the magnetic moment has changed over time by comparing to the 2020 G-2 white paper, and the 2021 BMW correction including lattice QCD corrections [15, 11].

Additionally, we include a comparison with the allowable coupling of a heavy photon calculated from $(g-2)_e$ using precision measurements of α from Cs and Rb measurements, noting small exclusions of the preferred ATOMKI coupling solely from the two measurements [16, 17]. This study discusses the viability of a vector boson at the ATOMKI mass and notes that only a sliver of overlap exists between current experimental constraints and a protophobic vector boson within the preferred ATOMKI region [14]. The model of interest for a vector boson must also have neutrino suppression. This study focuses on this vector model interpretation, though the author recognizes the pseudo-scalar interpretation has not been fully excluded in the ATOMKI favored region. For the purposes of this study, we do not overlay all experimental exclusions and visually only compare the favored ATOMKI bounds to allowed ϵ_ℓ from each $(g-2)_\ell$, the reported PADME upperlimit and the NA64 exclusion contour.

2 Current Values of the Δa_μ and Δa_e

2.1 Latest Experimental Measurement and Standard Model Predictions for a_μ

The anomalous magnetic moment of the muon,

$$a_\mu \equiv \frac{g_\mu - 2}{2}. \quad (6)$$

is a stringent test of the Standard Model (SM) and a sensitive probe for new physics. Recent advances in both experiment and theory have led to an updated assessment of the longstanding discrepancy Δa_μ

between measurement and the SM expectation. In this section, we summarize the latest values for a_μ and their uncertainties as of 2025, including both data-driven and lattice QCD evaluations of the hadronic vacuum polarization (HVP) contribution.

Discrepancy and Uncertainty Propagation

The discrepancy between experiment and theory is calculated as

$$\Delta a_\mu = a_\mu^{\text{exp}} - a_\mu^{\text{SM}} \quad (7)$$

with the uncertainty calculated by adding in quadrature:

$$\sigma_{\Delta a_\mu} = \sqrt{\sigma_{\text{exp}}^2 + \sigma_{\text{SM}}^2} \quad (8)$$

FNAL Final Experimental Average

As reported by the Muon $g - 2$ Collaboration, the final combined experimental (exp) average, from BNL E821 4 and Runs 1-6 [10].

$$a_\mu^{\text{exp}} = 116\,592\,0715\,(145) \times 10^{-11} \quad (9)$$

Standard Model (SM) Predictions of a_μ and Corresponding Δa_μ

- **Dispersive/Data-driven HVP (Muon $g - 2$ Theory Initiative, 2020)** To demonstrate how only the dispersive hadronic vacuum polarization influences the allowable parameter space that a dark, or heavy photon, we include the theory estimate from the 2020 (g-2) white paper [15]

$$a_\mu^{\text{SM,WP20}} = 116\,591\,810\,(43) \times 10^{-11} \quad (10)$$

$$\Delta a_\mu^{\text{WP20}} = a_\mu^{\text{exp}} - a_\mu^{\text{SM,WP20}} \quad (11)$$

$$= [116\,592\,071.5 - 116\,591\,810] \times 10^{-11} \quad (12)$$

$$= 261.5 \times 10^{-11} \quad (13)$$

$$\sigma_{\Delta a_\mu^{\text{WP20}}} = \sqrt{(14.5)^2 + 43^2} \times 10^{-11} \quad (14)$$

$$= \sqrt{210.25 + 1849} \times 10^{-11} \quad (15)$$

$$\approx 45.4 \times 10^{-11} \quad (16)$$

Thus,

$$\boxed{\Delta a_\mu^{\text{WP20}} = 262(45) \times 10^{-11}} \quad (17)$$

- **BMW Lattice QCD HVP (BMW Collaboration, 2021)** Including the 2021 calculations from the BMW collaboration, highlight the significant shrinking of allowed parameter space

$$a_\mu^{\text{SM,BMW}} = 116\,591\,954\,(67) \times 10^{-11} \quad (18)$$

$$\Delta a_\mu^{\text{BMW}} = a_\mu^{\text{exp}} - a_\mu^{\text{SM,BMW}} \quad (19)$$

$$= [116\,592\,071.5 - 116\,591\,954] \times 10^{-11} \quad (20)$$

$$= 117.5 \times 10^{-11} \quad (21)$$

$$\sigma_{\Delta a_\mu^{\text{BMW}}} = \sqrt{(14.5)^2 + 67^2} \times 10^{-11} \quad (22)$$

$$= \sqrt{4699.25} \times 10^{-11} \quad (23)$$

$$\approx 68.6 \times 10^{-11} \quad (24)$$

Thus,

$$\boxed{\Delta a_\mu^{\text{BMW}} = 118(69) \times 10^{-11}} \quad (25)$$

- **Muon $g - 2$ Theory Initiative, 2025:** Finally we use the latest theoretical predictions from the (G-2) theory initiative to create the latest allowable heavy photon bands.

$$a_\mu^{\text{SM}, \text{GWP}} = 116\,592\,033(630) \times 10^{-11} \quad (26)$$

$$\Delta a_\mu^{\text{WP25}} = a_\mu^{\text{exp}} - a_\mu^{\text{SM}, \text{GWP}} \quad (27)$$

$$= [116\,592\,071.5 - 116\,592\,033] \times 10^{-11} \quad (28)$$

$$= 38.5 \times 10^{-11} \quad (29)$$

$$\sigma_{\Delta a_\mu^{\text{WP25}}} = \sqrt{(14.5)^2 + 62^2} \times 10^{-11} \quad (30)$$

$$= \sqrt{4054.25} \times 10^{-11} \quad (31)$$

$$\approx 63.7 \times 10^{-11} \quad (32)$$

Thus,

$$\boxed{\Delta a_\mu^{\text{WP25}} = 39(64) \times 10^{-11}}$$

2.2 Anomalous Magnetic Moment of the Electron

Determining Δa_e from Precision α Measurements

The electron anomalous magnetic moment is defined as

$$a_e \equiv \frac{g_e - 2}{2}. \quad (33)$$

Experimentally, a_e is known with extremely high precision from trapped-electron measurements (Penning trap) [18, 19]. The Standard Model (SM) prediction can be written as

$$a_e^{\text{SM}}(\alpha) = a_e^{\text{QED}}(\alpha) + a_e^{\text{had}} + a_e^{\text{EW}}, \quad (34)$$

where a_e^{QED} is the perturbative QED series known through five loops, expressed as

$$a_e^{\text{QED}}(\alpha) = \sum_{n=1}^5 C_{2n} \left(\frac{\alpha}{\pi} \right)^n, \quad (35)$$

with coefficients C_{2n} given in Ref. [20, 21]. The small hadronic vacuum polarization, light-by-light term a_e^{had} and electroweak term a_e^{EW} are also included (see the consolidated SM evaluation in [21]). Because a_e^{QED} dominates and depends sensitively on α , different independent determinations of the fine structure constant yield different SM predictions $a_e^{\text{SM}}(\alpha_i)$, and hence different residuals

$$\Delta a_e^{(i)} \equiv a_e^{\text{exp}} - a_e^{\text{SM}}(\alpha_i). \quad (36)$$

We consider two recent, high-precision determinations of α :

1. The 2018 ^{133}Cs recoil measurement: $\alpha_{\text{Cs}18}^{-1} = 137.035\,999\,046(27)$ [16].
2. The 2020 ^{87}Rb recoil measurement: $\alpha_{\text{Rb}20}^{-1} = 137.035\,999\,206(11)$ [17].

Using a common set of higher-order QED, hadronic, and electroweak contributions (as compiled in [21]) and the experimental value, as determined by a one-electron quantum cyclotron,

$$a_e^{\text{exp}} = 0.001\,159\,652\,180\,59(13) \quad (37)$$

[22], the two SM predictions differ slightly due to the distinct α inputs. Propagating uncertainties (treating the α error, the experimental a_e error, and the SM theory truncation / hadronic / EW errors in quadrature), one obtains the residuals:

$$\Delta a_e^{(\text{Cs 2018})} = a_e^{\text{exp}} - a_e^{\text{SM}}(\alpha_{\text{Cs18}}) = -102(26) \times 10^{-10}, \quad (38)$$

$$\Delta a_e^{(\text{Rb 2020})} = a_e^{\text{exp}} - a_e^{\text{SM}}(\alpha_{\text{Rb20}}) = 34(16) \times 10^{-10}. \quad (39)$$

For each α_i we compute the uncertainties as

$$\sigma^2(\Delta a_e^{(i)}) = \sigma^2(a_e^{\text{exp}}) + \left(\frac{\partial a_e^{\text{SM}}}{\partial \alpha} \right)_{\alpha_i}^2 \sigma^2(\alpha_i) + \sigma_{\text{th,res}}^2, \quad (40)$$

where $\sigma_{\text{th,res}}$ encompasses the residual uncertainties (higher-order QED coefficient uncertainties, hadronic, and electroweak inputs). The derivative is dominated by the leading QED term:

$$\frac{\partial a_e^{\text{SM}}}{\partial \alpha} \simeq \frac{1}{\pi} C_2 + \frac{2}{\pi^2} C_4 \alpha + \dots, \quad (41)$$

with $C_2 = \frac{1}{2}$, $C_4 \approx 0.328478965 \dots$ etc. [20, 21]. In practice the full five-loop series is used numerically when producing Eqs. (38)–(39). The sign flip between the two Δa_e values arises because the Rb determination yields a slightly *larger* α^{-1} (smaller α) than the Cs value, shifting the QED prediction and thus the residual.

The two precision α measurements lead to electron anomaly residuals of opposite sign, Eqs. (38)–(39). Any global fit to new-physics explanations of magnetic moment data must therefore treat the Cs 2018 and Rb 2020 inputs as distinct scenarios.

3 Heavy Photon mixing with a lepton at Vacuum level

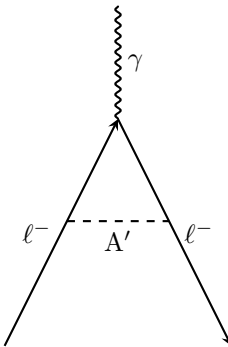


Figure 1: Leading-order heavy photon contribution to the gyromagnetic ratio of a lepton.

3.1 Calculating Leptonic Kinetic Mixing Parameters

In the minimal kinetic mixing (“dark/heavy photon”) scenario with Lagrangian

$$\mathcal{L} \supset -\frac{1}{4} F'_{\mu\nu} F'^{\mu\nu} - \frac{\varepsilon}{2} F'_{\mu\nu} B^{\mu\nu} + \frac{1}{2} m_{A'}^2 A'_\mu A'^\mu$$

the induced interaction after electroweak symmetry breaking is flavor universal,

$$\mathcal{L}_{\text{int}} \supset \varepsilon e \sum_f Q_f \bar{f} \gamma^\mu f A'_\mu,$$

thus the same kinetic mixing ε governs both (i) the one-loop correction to a_μ and a_e and (ii) production / decay into e^+e^- relevant for the nuclear transition ATOMKI anomaly.

The one-loop contribution of a light vector of mass $m_{A'}$ to a charged lepton anomalous moment is calculated using the form factor F_V where

$$\Delta a_\ell^{A'} = \frac{\alpha \varepsilon^2}{2\pi} F_V \left(\frac{m_{A'}}{m_\ell} \right), \quad F_V(r) = \int_0^1 dx \frac{2x(1-x)^2}{(1-x)^2 + r^2 x},$$

which yields the limiting forms $F_V(r \ll 1) \simeq 1$ and $F_V(r \gg 1) \simeq \frac{2}{3} \frac{m_\ell^2}{m_{A'}^2}$, allowing a direct mapping between a measured (or hypothesized) Δa_ℓ and the required ε [23].

Thus, the kinetic mixing parameter is

$$\varepsilon_\ell(m_{A'}) = \sqrt{\frac{\Delta a_\ell (2\pi/\alpha)}{F_V(m_{A'}/m_\ell)}} \quad (42)$$

Here, m_μ is the mass of the respective lepton, and α is the fine structure constant ($\alpha \approx 1/137$). The 1σ uncertainty on the kinetic mixing parameter ε_ℓ is propagated as:

$$\sigma_{\varepsilon_\ell} = \frac{1}{2} \frac{\varepsilon_\ell}{\Delta a_\ell} \sigma_{\Delta a_\ell} \quad (43)$$

where Δa_ℓ and $\sigma_{\Delta a_\ell}$ are the central value and uncertainty of the anomalous magnetic moment discrepancy, respectively.

At next-to-leading order the dark photon contribution acquires standard QED two-loop vertex and self-energy corrections. These dress the one-loop amplitude without introducing additional powers of ε . The corrected expression can be written

$$\Delta a_\ell^{A'} = \frac{\alpha \varepsilon^2}{2\pi} F_V(r) \left[1 + \frac{\alpha}{\pi} \delta_V(r) \right],$$

where F_V is given above and $\delta_V(r) = \mathcal{O}(1)$ encodes the finite two-loop terms (no large logarithms for $m_{A'} \sim \mathcal{O}(m_\ell)$).

$$\frac{\Delta a_\ell^{A',\text{NLO}} - \Delta a_\ell^{A',\text{LO}}}{\Delta a_\ell^{A',\text{LO}}} \sim \mathcal{O}\left(\frac{\alpha}{\pi}\right) \approx 2.3 \times 10^{-3}$$

Numerically, this modifies ε extracted from Δa_ℓ at the 10^{-3} relative level, negligible compared to the leading order uncertainties. Thus, leading order expressions suffice for the parameter-space contours presented here.

4 Current Feasibility of a 17 MeV Vector Boson

4.1 ATOMKI Measurements

The ATOMKI Collaboration first reported a $> 5\sigma$ anomaly in the internal pair-creation angular correlations for the 17.6 MeV M1 transition in ${}^8\text{Be}$, which can be interpreted as the emission of a new vector boson X17 with mass $m_{A'} = (16.7 \pm 0.85)$ MeV [12]. This collaboration repeated these studies and then performed additional experiments focused around the e^+e^- pair production of ${}^4\text{He}$ and ${}^{12}\text{C}$ nuclei. Respectively, the authors found similar excesses at large correlation angles with best-fit mass measurements of (17.01 ± 0.16) MeV, (16.94 ± 0.33) MeV, and (17.01 ± 0.31) MeV yielding a preferred kinetic mixing parameter in the range $\varepsilon_e \approx \times 10^{-4} - 10^{-3}$. [13, 24, 25]. For the purposes of this study, we consider the original ATOMKI mass of 16.7 MeV in the preferred range for $\varepsilon \in [2 \times 10^{-4}, 1.3 \times 10^{-3}]$ and preferred coupling to this as determined in [14].

4.2 Additional Experimental Constraints at 17 MeV

NA48/2 Exclusion and Protophobic Implication

The NA48/2 limit from the decay chain

$$\pi^0 \rightarrow \gamma A' \rightarrow \gamma e^+ e^-$$

imposes $\varepsilon^2 \lesssim 10^{-7} \Rightarrow \varepsilon \lesssim 3 \times 10^{-4}$ at $m_{A'} \simeq 16.7$ MeV. Therefore, any viable explanation of the ATOMKI excess must invoke a *protophobic* gauge boson: its effective coupling to protons (the relevant linear combination of u and d quark charges) is suppressed to evade the π^0 decay bound while retaining a sufficiently large coupling to electrons to generate the observed internal pair-creation anomaly[14].

NA64 at CERN and Neutrino Suppression

Complementary probes have already excluded large portions of this parameter space: the NA64 fixed-target search at CERN rules out $1.3 \times 10^{-4} \leq \varepsilon_e \leq 6.8 \times 10^{-4}$ at 90% CL for $m_{A'} = 16.7$ MeV [26], while beam-dump experiments (E141, E774), $e^+ e^-$ collider searches at BaBar and KLOE, and analyses by HADES, PHENIX, and NA48/2 constrain $\varepsilon^2 \lesssim 10^{-7}$ for $9 < m_{A'} < 70$ MeV.

Neutrino couplings and the applicability of NA64 limits.

For the 2017–2018 combined datasets, NA64 reports a 90% C.L. exclusion at

$$1.2 \times 10^{-4} < \varepsilon_e^{(\text{NA64})} < 6.8 \times 10^{-4}, \quad m_X = 16.7 \text{ MeV}, \quad (44)$$

where ε_e is the coupling of the new boson to electrons [27].

The NA64 “visible” exclusion in Eq. (44) is obtained under the benchmark assumption $\text{BR}(X \rightarrow e^+ e^-) = 1$ [28]. In a generic protophobic- X interpretation, however, the coupling to neutrinos is model-dependent. In particular, reactor CE ν NS data place strong bounds on ε_{ν_e} at $m_X \simeq 17$ MeV, requiring $|\varepsilon_{\nu_e}| \ll |\varepsilon_e|$ in viable ATOMKI-motivated scenarios. This implies that the low-energy lepton couplings cannot satisfy the naive $\text{SU}(2)_L$ relation between ε_{ν_e} and ε_e (e.g. $2\varepsilon_{\nu_e} = \varepsilon_e$ for purely vector couplings), i.e. an effective $\text{SU}(2)_L$ -relation violation in the lepton sector is required [7].

Motivated by this, in the remainder of this work we adopt a neutrino-coupling-suppressed benchmark,

$$|\varepsilon_{\nu_\alpha}| \ll |\varepsilon_e|, \quad \alpha = e, \mu, \tau, \quad (45)$$

and assume no additional light invisible states below $m_X/2$. In this regime $\text{BR}(X \rightarrow \nu \bar{\nu}) \simeq 0$, so the NA64 visible-decay exclusion Eq. (44) can be applied without further rescaling.

Optional rescaling for a nonzero invisible width. For completeness, if X has an invisible partial width (e.g. into neutrinos or other invisible states),

$$R \equiv \Gamma_{\text{inv}}/\Gamma_{e^+ e^-}, \quad \text{BR}_{ee} = \frac{1}{1+R}, \quad \Gamma_{\text{tot}} = \Gamma_{e^+ e^-}(1+R),$$

then the high- ε_e (prompt-decay) edge of the visible NA64 “bean” shifts approximately as

$$\varepsilon_e^{(\text{vis})} \rightarrow \frac{\varepsilon_e^{(\text{vis})}}{\sqrt{1+R}}, \quad (46)$$

While the low- ε_e (long-lived) edge is essentially unchanged up to small acceptance effects.

If BR_{inv} is sizeable, NA64’s missing-energy search for invisibly decaying dark photons provides an additional constraint [29]; reinterpreting that result in a given protophobic- X model requires specifying BR_{inv} and the promptness of the invisible decay. We do not apply this constraint in the benchmark neutrino-suppressed scenario of Eq. (45).

2025 PADME Observed Upper Limit and Coupling Conversion

Most recently, the PADME experiment performed a resonant search via e^+e^- annihilation on a fixed target, scanning $\sqrt{s} = 16.4\text{--}17.4$ MeV; the data showed a local upward fluctuation at $\sqrt{s} \approx 16.90$ MeV with a global significance of $\approx 1.8\sigma$ but no definitive signal, and set 90% CL upper limits on $g_{ve} \leq 5.6 \times 10^{-4}$ near the X17 mass [30].

PADME limit and coupling conversion. PADME quotes limits in terms of a direct vector coupling g_{ve} defined by

$$\mathcal{L} \supset g_{ve} X_\mu \bar{e} \gamma^\mu e. \quad (47)$$

[30] To compare with ε_e , we use $g_{ve} = e \varepsilon_e$, with $e \equiv \sqrt{4\pi\alpha_{\text{em}}}$, i.e.

$$\varepsilon_e = \frac{g_{ve}}{e}. \quad (48)$$

PADME reports that the observed 90% C.L. upper-limit curve is weakest near $M_X = 16.90$ MeV with a corresponding global significance of $\approx 1.8\sigma$ and reaches $g_{ve}^{90} \simeq 5.6 \times 10^{-4}$ [30], corresponding to

$$\varepsilon_e^{(\text{PADME})}(16.90 \text{ MeV}) \lesssim \frac{5.6 \times 10^{-4}}{e} \simeq 1.9 \times 10^{-3}. \quad (49)$$

Unexcluded interval (NA64 visible + PADME). Combining Eqs. (44) and (49), the coupling interval

$$6.8 \times 10^{-4} \lesssim \varepsilon_e \lesssim 1.9 \times 10^{-3} \quad (m_X \simeq 16.9 \text{ MeV}) \quad (50)$$

is not excluded by the NA64 displaced-decay search and the PADME resonant-production limit. The lower endpoint corresponds to the high- ε_e edge of the NA64 “visible” bean, where the NA64 acceptance rapidly drops for promptly decaying $X \rightarrow e^+e^-$. This region is further excluded by the Rb2020 measurements as will be shown in the results section.

The PRad-II/X17 collaboration and the Hall B X17 search concept

Some studies exist that have focused on PIONEER and Mu3e as promising experimental tests to probe the X17 parameter space [31]. Another exciting prospect is the planned Hall B “X17 Search Experiment” at Thomas Jefferson National Accelerator Facility (JLAB). This experiment is being pursued by the PRad-II/X17 collaboration, with co-spokespersons including A. Gasparian, R. Paremuyan, D. Dutta, N. Liyanage, Ch. Peng, H. Gao, and T. Hague [32]. The collaboration’s near-term physics goal is twofold: (i) to validate (or set an upper limit on) electroproduction of the putative ~ 17 MeV state reported by ATOMKI, and (ii) to search more broadly for hidden-sector intermediate states in the $m_X \in [3, 60]$ MeV range that decay to e^+e^- and/or $\gamma\gamma$ [32].

Experimentally, the strategy is a forward-angle, fully-exclusive invariant-mass resonance search “bump hunt” in $e^- + \text{Ta} \rightarrow e^- + A' + \text{Ta} \rightarrow e^- + e^+e^- + \text{Ta}$, using a very thin heavy target (baseline $\sim 1 \mu\text{m}$ Ta) and detecting all final-state particles to tightly constrain kinematics [32, 33]. The detector apparatus is a magnetic-spectrometer-free configuration derived from the PRad setup on the Hall B space frame upstream of CLAS12, combining the high-resolution PbWO₄ inner section of the HyCal electromagnetic calorimeter with two GEM tracking layers [32, 33]. In this design, the calorimeter provides precise energy measurements and triggering, while the GEMs enable charged/neutral discrimination and rejection of non-target backgrounds (e.g. tracks originating from beamline material), enabling powerful exclusivity selections (energy consistency and coplanarity) [32, 33]. The collaboration reports a target-constrained invariant-mass resolution of order $\sigma_m \simeq 0.48$ MeV for an $m_X \simeq 17$ MeV hypothesis, and emphasizes a complementary “unconstrained” reconstruction as a cross-check that any peak-like excess originates from the target; the setup is not intended as a displaced-vertex search [32].

Recent status

By the June 2025 collaboration update, PRad-II and X17 had passed an Experiment Readiness Review (ERR) in May (with recommendations/comments to be addressed), and a preliminary installation/run schedule was presented with PRad-II commissioning and running preceding an X17 running window in May–July 2026 [33]. The same update reports progress on beamline and detector components (including HyCal channel testing and GEM construction/shipping milestones) consistent with an on-track path to the planned run period [33].

5 Results

5.1 Determining ε_μ using Δa_μ

Following the prescription of **Section 3.1** we calculate the kinetic mixing parameter, ε_μ , for heavy photon masses, m_X within the range [5, 500] MeV for three theoretical scenarios. The calculated values for a subset within this range are listed in Table 1 and explicitly plotted in 2.

As an example, and to compare with the ATOMKI measurement, suppose $m_{A'} = 17$ MeV. We have $r \approx 0.161$ and $f(r) \approx 0.68$. Taking the latest values:

$$\begin{aligned}\Delta a_\mu^{\text{disp}} &= 262(45) \times 10^{-11} \quad (\text{WP 2020}) \\ \Delta a_\mu^{\text{BMW}} &= 118(69) \times 10^{-11} \quad (\text{BMW 2021})\end{aligned}$$

we obtain:

$$\varepsilon_\mu^{\text{disp}} = \sqrt{\frac{262 \times 10^{-11} \cdot (2\pi/\alpha)}{0.68}} \approx 1.82 \times 10^{-3}$$

and

$$\varepsilon_\mu^{\text{BMW}} = \sqrt{\frac{118 \times 10^{-11} \cdot (2\pi/\alpha)}{0.68}} \approx 1.22 \times 10^{-3}$$

Therefore, the original muon- $(g-2)$ -favored kinetic mixing,

$$\varepsilon_\mu^{\text{disp}} \approx 1.82 \times 10^{-3},$$

shrinks to

$$\varepsilon_\mu^{\text{BMW}} \approx 1.22 \times 10^{-3}$$

once BMW lattice corrections are included, moving the central value of the allowable coupling strength within the ATOMKI X17 preferred range of

$$2 \times 10^{-4} \leq |\varepsilon| \leq 1.4 \times 10^{-3}$$

for a 16.7 MeV boson [14]. The (g-2) theory initiative 2025 white paper then narrows the central value to the allowable coupling further, where

$$\Delta a_\mu^{\text{WP25}} = 39(64) \times 10^{-11}$$

corresponding to

$$\varepsilon_\mu^{\text{WP25}} = 7.034 \times 10^{-4}$$

These three theoretical predictions for allowed coupling on ε with corresponding 1σ and 2σ contours are overlayed with the ATOMKI X17 parameter band in Figure 3. Table 1 provides the computations for a subset of hypothetical vector boson masses within the range [5, 500] MeV.

Mass [MeV]	$\varepsilon_{\text{WP20}}$	$\sigma(\varepsilon_{\text{WP20}})$	ε_{BMW}	$\sigma(\varepsilon_{\text{BMW}})$	$\varepsilon_{\text{WP25}}$	$\sigma(\varepsilon_{\text{WP25}})$
5	1.604e-03	1.377e-04	1.076e-03	3.146e-04	6.187e-04	5.077e-04
10	1.698e-03	1.458e-04	1.139e-03	3.331e-04	6.549e-04	5.374e-04
15	1.788e-03	1.535e-04	1.200e-03	3.508e-04	6.897e-04	5.659e-04
17	1.823e-03	1.566e-04	1.223e-03	3.577e-04	7.034e-04	5.771e-04
20	1.875e-03	1.611e-04	1.259e-03	3.680e-04	7.236e-04	5.937e-04
25	1.962e-03	1.685e-04	1.316e-03	3.849e-04	7.568e-04	6.210e-04
30	2.047e-03	1.758e-04	1.373e-03	4.016e-04	7.896e-04	6.479e-04
35	2.131e-03	1.830e-04	1.430e-03	4.181e-04	8.220e-04	6.745e-04
40	2.214e-03	1.901e-04	1.486e-03	4.344e-04	8.542e-04	7.009e-04
45	2.297e-03	1.972e-04	1.541e-03	4.507e-04	8.862e-04	7.271e-04
50	2.379e-03	2.043e-04	1.597e-03	4.668e-04	9.180e-04	7.532e-04
100	3.192e-03	2.741e-04	2.142e-03	6.263e-04	1.231e-03	1.010e-03
200	4.812e-03	4.132e-04	3.229e-03	9.441e-04	1.856e-03	1.523e-03
300	6.448e-03	5.538e-04	4.327e-03	1.265e-03	2.488e-03	2.041e-03
400	8.101e-03	6.957e-04	5.437e-03	1.590e-03	3.126e-03	2.565e-03
500	9.768e-03	8.389e-04	6.555e-03	1.917e-03	3.769e-03	3.092e-03

Table 1: Calculated kinetic mixing parameter ε_μ (and 1σ uncertainties) for three scenarios [dispersive only (“WP20”), BMW lattice 2021 calculations (“BMW”), and 2025 white paper (“WP25”)] using the final FNAL average a_μ^{exp} , for a subset of hypothetical vector boson masses within the range [5, 500] MeV.

5.2 Determining ε_e using Δa_e

Although we don’t explicitly make a table for a range of selections that could be allowable for Δa_e , the central values for ε_e when $m_{A'} = 17$ MeV are.

$$\varepsilon_e^{\text{CS18}} = 1.19(15) \times 10^{-3} \quad (51)$$

$$\varepsilon_e^{\text{RB20}} = 0.69(15) \times 10^{-3} \quad (52)$$

Given the vector interpretation necessitating a positive value of Δa_e , we only plot the mean $\varepsilon_e^{\text{CS18}}$ (using $|\Delta a_e|$) alongside the 1σ and 2σ favored regions about $\varepsilon_e^{\text{RB20}}$ as calculated for masses $m_{A'} \in [5, 50]$ MeV. This is plotted alongside the 1σ and 2σ allowed ε_μ and the ATOMKI/NA64 observed limits in 2.

6 Conclusion

This work re-evaluates whether a kinetically mixed dark photon, A' , can reconcile the muon and electron magnetic-moment anomalies with the nuclear e^+e^- excess reported by ATOMKI at 17, MeV. The final 2025 Fermilab $(g-2)_\mu$ result, together with the BMW21 lattice and WP25 theory updates, plays a central role in reassessing the favored kinetic-mixing parameter ε .

Impact of the 2025 $(g-2)_\mu$ determination. Using the same experimental input but three successive theory treatments, the preferred muonic coupling has moved steadily downward:

$$\varepsilon_\mu^{\text{WP20}} = 1.82 \times 10^{-3}, \quad \varepsilon_\mu^{\text{BMW21}} = 1.22 \times 10^{-3}, \quad \varepsilon_\mu^{\text{WP25}} = 7.03 \times 10^{-4}. \quad (53)$$

The reduction reflects improved control of hadronic vacuum-polarisation contributions; each refinement narrows the viable parameter space by roughly a factor of two.

For the electron, the one-electron quantum cyclotron combined with the Cs and Rb recoil determinations of the fine-structure constant leads to a $(g-2)_e$ residual that prefers a slightly smaller mixing with the following means:

$$\varepsilon_e^{\text{CS18}} = 1.19 \times 10^{-3}, \quad \varepsilon_e^{\text{RB20}} = 6.91 \times 10^{-4} \quad (54)$$

We recognize that the CS18 value is not to be considered in preferred coupling given the negative value of Δa_e (as vector bosons necessarily have a positive contribution to the ratio) and thus conclude with the RB20 value. At the X17 mass, the Rb20 electron preferred band and the muon exclusion band still overlaps at the 2σ level, so a universal (or mildly non-universal) A' interpretation remains possible.

Overlaying the leptonic constraints with the ATOMKI signal region yields the viable search range of

$$6.8 \times 10^{-4} \lesssim \epsilon \lesssim 9.6 \times 10^{-4}, \quad (55)$$

where the bottom of the range is given by NA64 and the max value of the range corresponds to the 2σ upper bound consistent with the favored electron coupling region from the 2020 Rb measurement. This region remains consistent with a protophobic gauge boson that satisfies the NA48/2 $\pi^0 \rightarrow \gamma A'$ bound. The window is narrow but not yet excluded.

PIONEER, Mu3e, and X17@JLAB are positioned to probe the remaining viable parameter space. The results of these programs will determine if anything in this parameter space corresponds to physics beyond the Standard Model or must be ruled out. In either case, the forthcoming results will decisively clarify the role of light vector bosons in the sub-GeV sector and test the validity of the ATOMKI claims.

7 Acknowledgements

The author thanks Joseph Bailey and Aidan Hsu for discussions on existing exclusions and assistance in finding contours. The author thanks Anthony Morales for the discussions in helping clarify allowable leptonic coupling modes. The author is grateful for the many fruitful discussions with Andrew McEntaggert on Lattice QCD and explicit analytic forms. The author also thanks Rory O'Dwyer for double-checking calculations. AI was used as a tool for typesetting and formatting; all scientific content was created and validated by the author.

References

- [1] Pierre Fayet. The fifth interaction in grand-unified theories: A new force acting mostly on neutrons and particle spins. *Physics Letters B*, 172:363, 1986.
- [2] Pierre Fayet. The fifth force charge as a linear combination of baryonic, leptonic (or $b - l$) and electric charges. *Physics Letters B*, 227(1):127–132, 1989.
- [3] Pierre Fayet. Extra $u(1)$'s and new forces. *Nuclear Physics B*, 347(3):743–768, 1990.
- [4] Pierre Fayet. The light u boson as the mediator of a new force, coupled to a combination of q , b , l and dark matter. *The European Physical Journal C*, 77:53, 2017.
- [5] A. J. Krasznahorkay et al. Observation of anomalous internal pair creation in ${}^8\text{Be}$: A possible indication of a light, neutral boson. *Physical Review Letters*, 116:042501, 2016.
- [6] Jonathan L. Feng, Bartosz Fornal, Iftah Galon, Susan Gardner, Jordan Smolinsky, Tim M. P. Tait, and Philip Tanedo. Protophobic fifth-force interpretation of the observed anomaly in ${}^8\text{Be}$ nuclear transitions. *Physical Review Letters*, 117:071803, 2016.
- [7] Peter B. Denton and Julia Gehrlein. Neutrino constraints and the atomki x17 anomaly. *Physical Review D*, 108:015009, 2023.
- [8] Pierre Fayet. u -boson production in e^+e^- annihilations, ψ and ν decays, and light dark matter. *Physical Review D*, 75:115017, 2007.
- [9] Maxim Pospelov. Secluded $u(1)$ below the weak scale. *Physical Review D*, 80:095002, 2009.
- [10] Muon $g-2$ Collaboration. Measurement of the positive muon anomalous magnetic moment to 127 ppb. 2025.

- [11] S. Borsanyi, Z. Fodor, J. N. Guenther, R. Kara, S. D. Katz, P. Parotto, C. Ratti, K. K. Szabo, C. Török, J. H. Wang, et al. Leading hadronic vacuum polarization contribution to the muon magnetic moment from lattice qcd. *Nature*, 593:51–55, 2021.
- [12] A. J. Krasznahorkay, M. Csatlós, L. Csige, J. Gulyás, M. Koszta, B. Szihalmi, J. Timár, Zs. Török, A. M. Nagy, N. Sas, et al. Observation of anomalous internal pair creation in ${}^8\text{Be}$: A possible indication of a light, neutral boson. *Phys. Rev. Lett.*, 116:042501, 2016.
- [13] A. J. Krasznahorkay, M. Csatlós, L. Csige, J. Gulyás, M. Hunyadi, M. Koszta, A. M. Nagy, N. Sas, J. Timár, Zs. Török, et al. New results for the ${}^8\text{Be}$ anomaly. *PoS*, BORMIO2019:036, 2019.
- [14] Jonathan L. Feng, Bartosz Fornal, Iftah Galon, Susan Gardner, Jordan Smolinsky, Tim M. P. Tait, and Philip Tanedo. Protophobic fifth-force interpretation of the observed anomaly in ${}^8\text{Be}$ nuclear transitions. *Phys. Rev. Lett.*, 117:071803, Aug 2016.
- [15] T. Aoyama et al. The anomalous magnetic moment of the muon in the standard model. *Phys. Rept.*, 887:1–166, 2020.
- [16] Richard H. Parker, Chenghui Yu, Wei Zhong, Brian Estey, and Holger Müller. Measurement of the fine-structure constant as a test of the standard model. *Nature*, 561:516–520, 2018.
- [17] Luc Morel, Zhibin Yao, Pierre Cladé, and Saïda Guellati-Khélifa. Determination of the fine-structure constant with an accuracy of 81 parts per trillion. *Nature*, 588:61–65, 2020.
- [18] D. Hanneke, S. Fogwell, and G. Gabrielse. New measurement of the electron magnetic moment and the fine structure constant. *Phys. Rev. Lett.*, 100:120801, 2008.
- [19] D. Hanneke, S. Fogwell Hoogerheide, and G. Gabrielse. Cavity control of a single-electron quantum cyclotron: Measuring the electron magnetic moment. *Phys. Rev. A*, 83:052122, 2011.
- [20] T. Aoyama, M. Hayakawa, T. Kinoshita, and M. Nio. Complete tenth-order qed contribution to the muon g-2. *Phys. Rev. Lett.*, 109:111807, 2012.
- [21] T. Aoyama, M. Hayakawa, T. Kinoshita, and M. Nio. The tenth-order qed contribution to the lepton g-2: Evaluation of dominant α^5 terms of muon g-2. *Phys. Rev. D*, 100:016012, 2019.
- [22] X. Fan, T. G. Myers, B. A. D. Sukra, and G. Gabrielse. Measurement of the electron magnetic moment. *Phys. Rev. Lett.*, 130:071801, Feb 2023.
- [23] Maxim Pospelov. Secluded $u(1)$ below the weak scale. *Phys. Rev. D*, 80:095002, 2009. Contains the A' one-loop $(g-2)_\ell$ integral $\int_0^1 dz \frac{2z(1-z)^2}{(1-z)^2 + (m_{A'}^2/m_\ell^2)z}$.
- [24] A. J. Krasznahorkay, M. Csatlós, L. Csige, J. Gulyás, A. Krasznahorkay, B. M. Nyakó, I. Rajta, J. Timár, I. Vajda, and N. J. Sas. New anomaly observed in ${}^4\text{He}$ supports the existence of the hypothetical x17 particle. *Phys. Rev. C*, 104:044003, Oct 2021.
- [25] A. J. Krasznahorkay, A. Krasznahorkay, M. Begala, M. Csatlós, L. Csige, J. Gulyás, A. Krakó, J. Timár, I. Rajta, I. Vajda, and N. J. Sas. New anomaly observed in ${}^{12}\text{C}$ supports the existence and the vector character of the hypothetical x17 boson. *Phys. Rev. C*, 106:L061601, Dec 2022.
- [26] D. et. al. Banerjee. Search for a Hypothetical 16.7 MeV Gauge Boson and Dark Photons in the NA64 Experiment at CERN. *Phys. Rev. Lett.*, 120(23):231802, 2018.
- [27] NA64 Collaboration. Improved limits on a hypothetical X(16.7) boson and a dark photon decaying into e^+e^- pairs. *Phys. Rev. D*, 101:071101, 2020.
- [28] D. Banerjee et al. Improved limits on a hypothetical x(16.7 mev) boson and a dark photon decaying into e^+e^- pairs. *Phys. Rev. Lett.*, 125:081801, 2020.

- [29] NA64 Collaboration. Search for Light Dark Matter with NA64 at CERN. *Phys. Rev. Lett.*, 131:161801, 2023.
- [30] F. Bossi, R. De Sangro, C. Di Giulio, E. Di Meco, D. Domenici, G. Finocchiaro, L. G. Foggetta, M. Garattini, P. Gianotti, M. Mancini, I. Sarra, T. Spadaro, C. Taruggi, E. Vilucchi, K. Dimitrova, S. Ivanov, K. Kostova, V. Kozhuharov, R. Simeonov, F. Ferrarotto, E. Leonardi, P. Valente, E. Long, G. C. Organtini, M. Raggi, and A. Frankenthal. Search for a new 17 MeV resonance via e^+e^- annihilation with the PADME Experiment. *arXiv preprint arXiv:2505.24797*, 2025.
- [31] Luca Di Luzio, Paride Paradisi, and Nudžejim Selimović. Hunting for a 17 mev particle coupled to electrons. *Nuclear Physics B*, 1021:117177, December 2025.
- [32] Ashot Gasparian. X17 search experiment in hall b: “a direct detection search for hidden sector new particles in the 3–60 mev mass range”. Slides presented at the HPS Collaboration Meeting, Jefferson Lab (Newport News, VA), for the PRad-II/X17 Collaboration, June 2024. PDF slides: [Gasparian_HPS_ColabMeeting_June_2024.pdf](#).
- [33] Rafayel Paremuzyan. Upcoming x17 experiment in hall b, jlab. Slides presented at the HPS Collaboration Meeting, Jefferson Lab (Newport News, VA), June 2025. PDF slides: [HPS_CollaborationMeeting_June_2025.pdf](#).

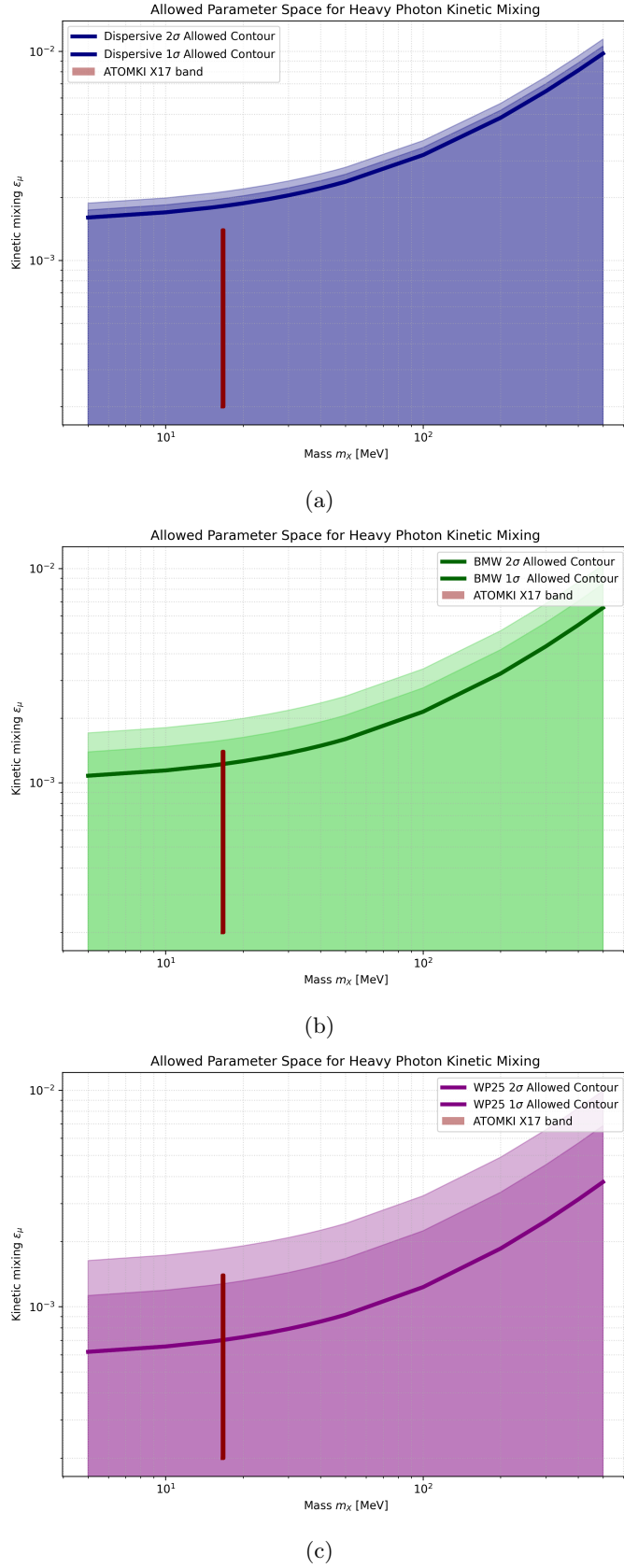


Figure 2: Comparison of $(g - 2)_\mu$ allowed parameter space using: WP20 (a), BMW21 (b), and WP25 (c) theory predictions.

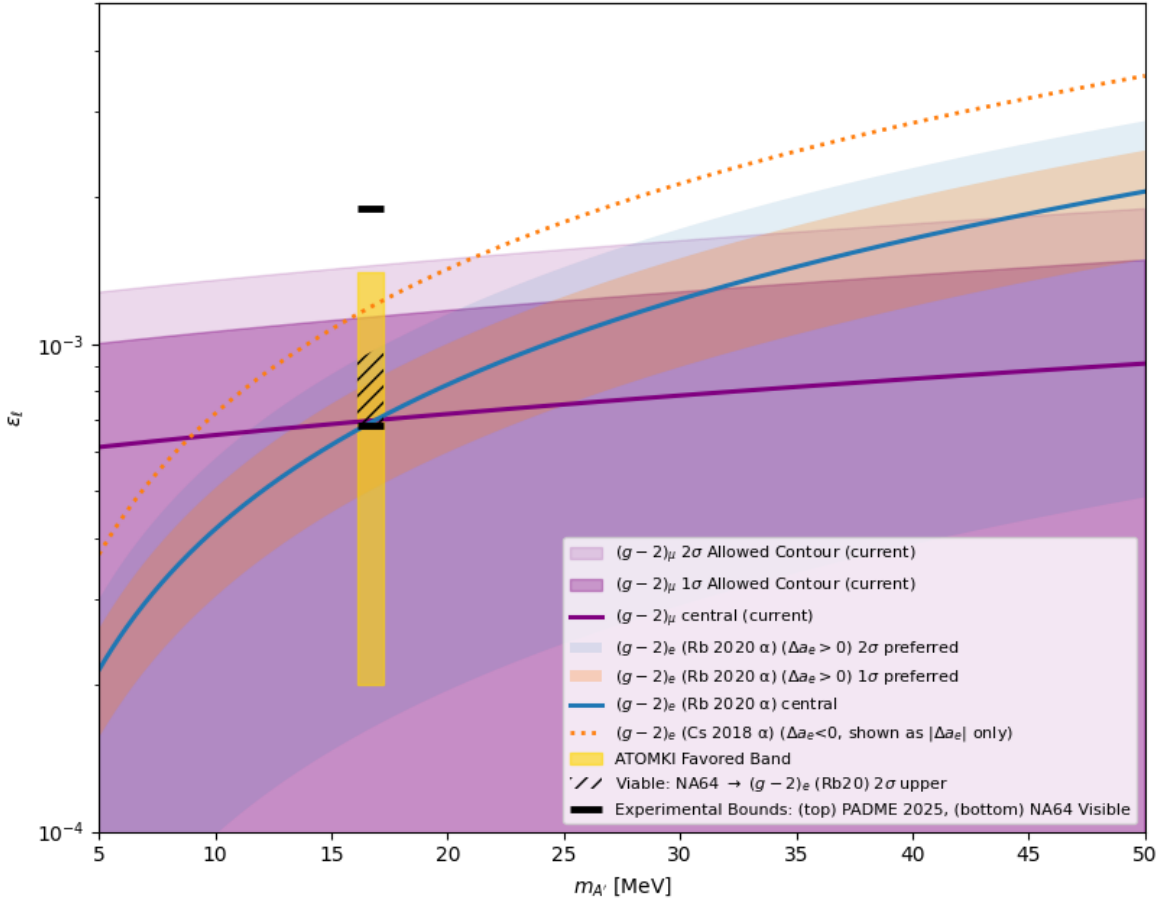


Figure 3: Overlay of ATOMKI preferred ε_e (yellow box) and allowable 1 σ , 2 σ contours on ε_e , ε_μ from fine structure precision measurements on the ^{87}Rb , ^{133}Cs and the FNAL final average a_μ respectively. The black lines indicate the current limits set by (top) PADME, and (bottom) NA64. In between the NA64 limit and the top of the 2 σ favored ε_e^{Rb20} band is the region still viable for the protophobic and neutrino-coupling suppressed interpretation of X17.